Model-independent X-ray Imaging of Adsorbed Cations at the Crystal-Water Interface

Z. Zhang,[1,2] P. Fenter,[1] L. Cheng,[1] N.C. Sturchio,[1,3] M.J. Bedzyk,[1,2]
M.L. Machesky,[4] D.J. Wesolowski[5]
[1]Argonne National Laboratory, Argonne, IL, U.S.A.
[2]Institute for Environmental Catalysis, Northwestern University, Evanston, IL, U.S.A.
[3]University of Illinois at Chicago, Chicago, IL, U.S.A.
[4]Illinois Water Survey, Champaign, IL, U.S.A.
[5]Oak Ridge National Laboratory, Oak Ridge, TN, U.S.A.

Introduction

Direct knowledge of solid-liquid interface structure is critically needed to understand many natural and technological processes [1]. The electrical double layer (EDL) [1, 2] can be described as a partitioning of ions between the adsorbed (Stern) and diffuse layers. The lack of direct knowledge concerning Stern layer structure substantially impedes a fundamental understanding of EDL phenomena. The ability to *directly* observe cation adsorption sites at the oxide-liquid interface is strongly limited because the existing holographic techniques have characteristics that make them inappropriate for imaging atomic distributions at the solid-liquid interface. Here, we describe a new approach to *directly* image 3-D elemental distributions of cations at the crystal-liquid interface [3].

Methods and Materials

Details of experimental procedures and solution conditions are described elsewhere [4]. Briefly, α-TiO_2 (rutile) (110) surfaces were exposed to dilute solutions of metal cations Sr^{2+}, Zn^{2+}, and Y^{3+}. These cations are observed to specifically adsorb from aqueous electrolyte solutions at 25°C, with a pH of ~6 to 11 and $[Me^{z+}]_{aq}$ of $<10^{-4}$ M.

An x-ray standing wave (XSW) is formed by coherent superposition of incident and Bragg-reflected x-ray beams, both above and below the surface of a perfect (or nearly perfect) crystal [5-8]. Measurements of the characteristic x-ray fluorescence as a function of incident angle at the H = hkl Bragg reflection (with Bragg plane spacing d_H) reveal the H^{th} Fourier coefficient F_H of the element-specific normalized density profile $\rho(r)$ (including both its amplitude f_H and phase P_H, also referred to as the coherent fraction and position, respectively). In other words [3, 4]:

$$F_H = \int \rho(r) \exp(i2\pi H \bullet r) dr$$

$$= f_H \exp(i2\pi P_H) \text{ [3,4] .}$$

Coherent positions and fractions for different reflections are determined by comparing the angular variation of the Bragg reflectivity and x-ray fluorescence signals with calculations using dynamical diffraction theory. This analysis does not impose any assumptions on the derived structure, since it relies only on information about the substrate crystal structure and the incident x-ray beam properties.

With the XSW imaging approach, the full elemental distribution $\rho(r)$ is obtained simply and directly by Fourier inversion of the XSW-measured Fourier coefficients:

$$\rho(r) = \mathrm{Re}[\Sigma_H F_H \exp(-2\pi i H \cdot r)]$$

$$= \mathrm{Re}[\Sigma_H f_H \exp(2\pi i(P_H - H \cdot r)] \text{ .}$$

This approach is robust as long as a sufficiently complete set of F_H coefficients is measured by XSW. This principle was recently established in the measurement of 1-D impurity distributions within a bulk crystal lattice [9]. This has also been applied to an ultrahigh-vacuum (UHV) surface adsorbate phase [10]. Such images cannot be generated so simply by conventional diffraction techniques because the phases P_H are not directly measured.

Results and Discussion

Full 3-D model-independent images of the elemental distributions are obtained with the measured coherent fractions and positions, with the rutile (110) surface symmetry used for symmetry-equivalent reflections. Slices through the derived 3-D distributions at the plane of maximum density are shown for Ti (from the substrate crystal) and the adsorbed ions (Fig. 1a). The derived Ti distribution clearly shows two locations within the surface unit cell that correspond to Ti directly bonded to bridging oxygen (BO) sites along [001] and to Ti directly below the terminal oxygen (TO) in the Ti-O plane. Sr^{2+} and Y^{3+} ions are revealed to be adsorbed at a “tetradentate” site

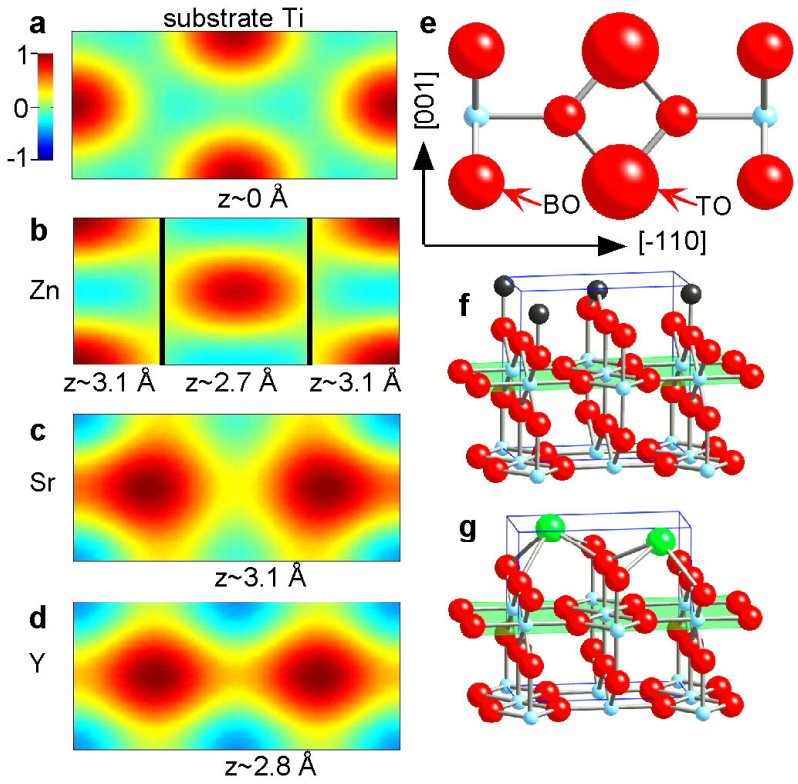

FIG. 1. (a-d) Measured lateral distributions of Ti (from the TiO_2 substrate) and of cations Zn^{2+}, Sr^{2+}, and Y^{3+} adsorbed to rutile shown as a cut through the plane of maximum density, whose height above the Ti-O plane (shaded in green in f and g) is indicated below each image. Part e gives a perspective view from above the rutile surface unit cell (oxygen in red, titanium in blue). Schematic adsorption geometries are shown for (f) Zn^{2+} and (g) Sr^{2+} and Y^{3+} in perspective 3-D views of the rutile-water interface.

between two TO sites and two BO sites, with differences in their heights controlled primarily by ion radii. In contrast, Zn^{2+} is adsorbed at two distinct sites (each at a different height), primarily above a single BO and, to a lesser extent, in a bidentate adsorption site between TOs. These Zn^{2+} sites are both close to the projected Ti lattice sites and therefore can be qualitatively understood as being due to the similarity of Zn and Ti ionic radii.

The intrinsic resolution of this approach corresponds to $d_{H\max}/2$, where $H_{\max}$ is the highest-order reflection along a particular direction H [8], so that the present data provide a full 3-D image of the ion distributions with a resolution of ~1 Å. The derived Ti distribution is dominated by the experimental resolution. In contrast, the adsorbate distributions exhibit some additional broadening (e.g., along [001] for Sr and [-110] for Zn), suggesting that the actual distributions may include either static or dynamic displacements from the nominal adsorption sites described above.

Bragg-XSW images of surface-adsorbed species, described here, project 3-D ion distributions into the primitive substrate crystallographic unit cell and therefore emphasize the Stern ion locations over the diffuse ion distribution. This also results in the well-known modulo-d_H ambiguity in the derived adsorbate position [5, 6]. With additional information (e.g., x-ray reflectivity data, molecular dynamics simulations), however, we demonstrated that each measured adsorbate species occurs as an inner-sphere adsorbate bonding directly to the rutile surface lattice [4].

This new model-independent image-based analysis of XSW data illustrated its ability to directly resolve the two distinct Zn^{2+} adsorption sites in a manner that is no more difficult than determining the substrate atom locations or the simpler distributions for Sr^{2+} and Y^{3+}. In systems where there may be co-adsorption of two or more species (e.g., ternary sorption complexes), the elemental sensitivity of XSW allows the distributions of each element to be determined in the same manner as that described above, as long as those elements are spectroscopically resolved (e.g., by their respective characteristic emissions).

Acknowledgments

This work was performed at BESSRC beamline station 12-ID-D at the APS and beamline X15A at the National Synchrotron Light Source. Use of both sources was supported by the U.S. Department of Energy, Office of Science, Office of Basic Energy Sciences, under Contract No. W-31-109-ENG-38. This report was extracted from Ref. 3.

References

[1] G.E. Brown, Jr. et al., Chem. Rev. **99**, 77-174 (1999).
[2] J. Lyklema, *Fundamentals of Interface and Colloid Science*, Vol. II (Academic Press, New York, NY, 1995).
[3] Z. Zhang, P. Fenter, L. Cheng, N.C. Sturchio, and M.J. Bedzyk, Surf. Sci. Lett. (in press, 2003)
[4] Z. Zhang, P. Fenter, L. Cheng, N.C. Sturchio, M.J. Bedzyk, M. Předota, A. Bandura, J. Kubicki, S.N. Lvov, P.T. Cummings, A.A. Chialvo, M.K. Ridley, P. Bénézeth, L. Anovitz, D.A. Palmer, M.L. Machesky, and D.J. Wesolowski (submitted, Langmuir 2003).
[5] J. Zegenhagen, Surf. Sci. Rep. **18**, 199-271 (1993) and references therein.
[6] M.J. Bedzyk, L. Cheng, Rev. Mineral. Geochem. **49**, 221-266 (2002) and references therein.
[7] B.W. Batterman, Phys. Rev. Lett. **22**, 703-705 (1969).
[8] J.A. Golovchenko, J.R. Patel, D.R. Kaplan, P.L. Cowan, and M.J. Bedzyk, Phys. Rev. Lett. **49**, 560-563 (1982).
[9] L. Cheng, P. Fenter, M.J. Bedzyk, and N.C. Sturchio, Phys. Rev. Lett. **90**, 255503(1-4) (2003).
[10] J.S. Okasinski, D.A. Walko, C.-Y. Kim, and M.J. Bedzyk, Phys. Rev. B (submitted, 2003).